Mathematics

https://www.aimspress.com/journal/Math

AIMS Mathematics, 11(8): 25874–25896.
DOI: 10.3934/math.20261037
Received: 04 July 2026
Revised: 08 August 2026
Accepted: 13 August 2026
Published: 20 August 2026

Research article

A degree-one Vassiliev invariant for planar knotoids via 0-smoothing

Liang Liang[1], **Fangyu Jin**[1] **and Liyuan Ma**[2,*]

[1] School of Mathematics, Liaoning Normal University, Dalian 116029, China
[2] School of Mathematical Sciences, Dalian University of Technology, Dalian 116024, China

* **Correspondence:** Email: liyuan_ma@126.com.

Abstract: We introduce a smoothing-based Laurent polynomial invariant for oriented planar knotoids by combining affine index weights with endpoint winding data. For a planar knotoid diagram D, we first define an auxiliary ordered winding Laurent polynomial $H_D(x, y)$, whose summands record the affine index weight of each classical crossing together with the homology class of the associated lobe in the twice-punctured plane. We then apply 0-smoothing against the orientation at each crossing and define $F_D(x, y)$ by combining the resulting changes in $H_D(x, y)$ with a writhe correction. We prove that both $H_D(x, y)$ and $F_D(x, y)$ are invariant under planar isotopy and the classical Reidemeister moves performed away from the endpoints. We also determine their behavior under orientation reversal and mirror image and establish an additivity formula for $F_D(x, y)$ under the planar product, subject to the specified exterior region condition. To illustrate the information supplied by smoothing, we construct an infinite family of planar knotoids for which the affine index polynomial and $H_D(x, y)$ are independent of the parameter, whereas $F_D(x, y)$ distinguishes all members of the family. Finally, by extending $F_D(x, y)$ to singular planar knotoids through the Vassiliev skein relation, we prove that it is a finite-type invariant of degree exactly one. These results provide a connection between affine index methods, endpoint winding information, and smoothing operations in planar knotoid theory.

Keywords: knotoids; planar knotoids; polynomial invariants; Vassiliev invariants; 0-smoothing
Mathematics Subject Classification: 57K12, 57K14, 57K16

1. Introduction

Knotoids, introduced by Turaev [1], are equivalence classes of generic immersions of the oriented interval into an oriented surface, equipped with over/under information at double points and considered up to ambient isotopy and Reidemeister moves performed away from the endpoints. Throughout this paper, all diagrams are drawn in $\mathbb{R}^2$, and equivalences are taken to be oriented planar knotoid equivalences. In recent years, many polynomial invariants of knotoids have been constructed as generalizations of classical knot polynomials, such as the extended biquandle bracket polynomial [2] and quandle invariants for knotoids [3]. Turaev [1] showed that the set of classical knots embeds faithfully into the set of spherical knotoids and that classical invariants such as the Jones polynomial extend to knotoids. Gügümcü and Kauffman [4] extended classical knot and link invariants to knotoids in the sphere S^2. They also defined the affine index polynomial for knotoids and virtual knotoids, which is analogous to the corresponding invariants of virtual knots. Bataineh [5] introduced polynomial invariants of planar and spherical knotoids through the theory of polar knots. These invariants are derived as enhancements of the biquandle counting invariant. Henrich [6] introduced a polynomial invariant for virtual knots which vanishes for classical knots. Finite-type invariants for knotoids were studied directly by Manouras et al. [7], who extended knotoid invariants to singular knotoids by a Vassiliev skein relation. Several index-type invariants for knotoids have also been adapted from constructions in virtual knot theory, including the rotational bracket polynomial for Morse knotoids [8], the index polynomial, and the nth polynomial invariants for virtual knotoids [9]. Feng and Li [10] also introduced a polynomial invariant for knotoids using Gauss diagrams. Bataineh et al. [11] introduced a well-defined ordered pair of winding numbers. These numbers correspond to the leg and the head of the knotoid, respectively. This pair of winding numbers can be regarded as an element of the first homology group of the twice-punctured plane. Kutluay [12] generalized the Khovanov knot homology to knotoids, obtaining a triply graded homological invariant called winding homology. Its definition uses winding numbers of closed curves in $\mathbb{R}^2$. As shown in [1], the canonical embedding of $\mathbb{R}^2$ into S^2 induces a surjective map from planar knotoids to spherical knotoids. However, this map is not injective: A nontrivial planar knotoid may become trivial when regarded as a spherical knotoid. This fundamental distinction implies that planar and spherical knotoid theories form distinct frameworks.

In this paper, we consider knotoid diagrams in the plane $\mathbb{R}^2$. We first define an ordered winding Laurent polynomial $H_D(x, y)$ by combining the affine index weight of a classical crossing with the ordered pair $(l(c), h(c))$ of winding numbers of its lobe. We then apply 0-smoothing against the orientation at every crossing and define the associated polynomial $F_D(x, y)$. The polynomial $F_D(x, y)$ measures the change of the ordered winding data under local smoothing. We prove invariance under planar isotopy and the classical Reidemeister moves performed away from the endpoints, establish transformation formulas under orientation reversal and mirror image, prove a product formula, and show that $F_D(x, y)$ is a degree-one Vassiliev invariant in the crossing-change sense. We also compute an explicit family for which the affine index polynomial and H_D are independent of the parameter, and F_D distinguishes all members. In displayed formulas, we retain the full arguments $H_D(x, y)$ and $F_D(x, y)$; in running text, they may be suppressed after the first occurrence when no ambiguity can arise.

The winding signed sum polynomial of Bataineh et al. [11] is constructed from crossing signs and endpoint winding data. The polynomial $H_D(x, y)$ also incorporates the affine index weight, and $F_D(x, y)$ records the change of $H_D(x, y)$ under 0-smoothing.

This article does not establish that $H_D(x, y)$ or $F_D(x, y)$ is a specialization, weighted form, or linear combination of the winding signed sum polynomial. Accordingly, the comparison in Section 4.1 is restricted to the affine index polynomial and $H_D(x, y)$, and no general dominance over other planar knotoid invariants is claimed.

The paper is organized as follows. In Section 2, we recall the relevant definitions and basic results for knotoids. In Section 3, we introduce the ordered winding Laurent polynomial for planar knotoids, prove its invariance under Reidemeister moves, and discuss some properties of $H_D(x, y)$. In Section 4, we define $F_D(x, y)$ by applying the 0-smoothing operation, prove its invariance under Reidemeister moves, study its basic transformation and product properties, and give an explicit family illustrating its distinguishing power. In Section 5, we prove that $F_D(x, y)$ is a degree-one Vassiliev invariant. Finally, Section 6 summarizes the main conclusions and outlines several directions for further study.

2. Preliminaries

In this section, we recall the definitions and background needed for the constructions below. The basic theory of knotoids follows Turaev [1]. The affine index polynomial for knotoids is taken from Gügümcü and Kauffman [4]. Polynomial invariants of planar and spherical knotoids based on polar knots were studied by Bataineh [5]. The finite-type framework for knotoids and singular knotoids follows Manouras et al. [7]. The ordered endpoint winding pair used below was introduced by Bataineh et al. [11]. For additional background on knotoids and braidoids, we refer to Gügümcü et al. [13]. For local singular Reidemeister moves, we use the generating moves described by Bataineh et al. [14]. The smoothing and labeling conventions used in this paper are stated explicitly below.

Knotoids are oriented, knot-like objects that are conveniently represented by knotoid diagrams. A knotoid diagram is a generic immersion of the oriented interval $[0, 1]$ into an oriented surface, with over/under information assigned at each double point. The endpoints of a knotoid diagram, which are the images of 0 and 1, are distinct from each other and from the double points. They are called the leg and the head of the oriented knotoid diagram, respectively. The orientation of a knotoid diagram is from the leg to the head. In this paper, all diagrams are considered in $\mathbb{R}^2$. Figure 1 shows some oriented knotoid diagrams [13]. Geometrically, a planar knotoid diagram is a curve in the plane that crosses itself transversely at each classical crossing point. The crossing points are finite in number and isolated. Each classical crossing is a double point endowed with additional over/under information. The sign of a classical crossing c is defined as shown in Figure 2.

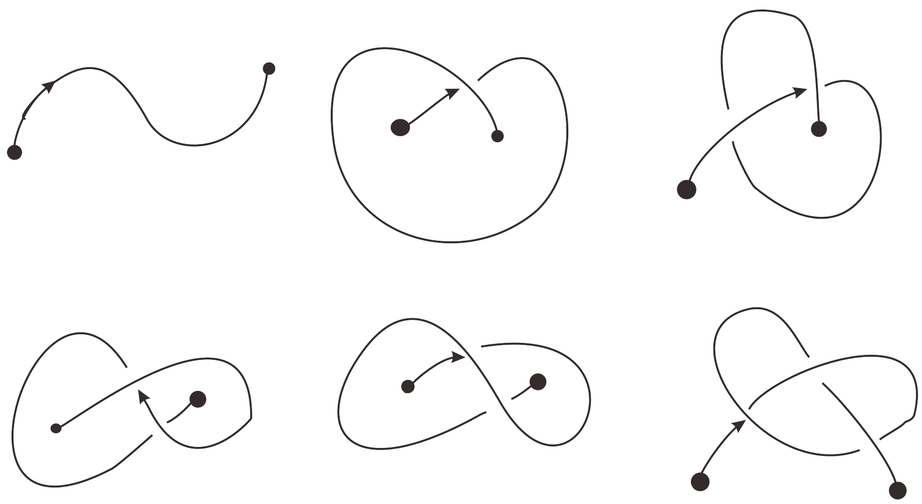

Figure 1. Some oriented knotoid diagrams.

Figure 2. The sign of a classical crossing c.

Definition 2.1. *([1]) Two oriented planar knotoid diagrams are equivalent if one can be deformed into the other by planar isotopy and a finite sequence of classical Reidemeister moves* R_1*,* R_2*, and* R_3 *away from the endpoints, as shown in Figure 3.*

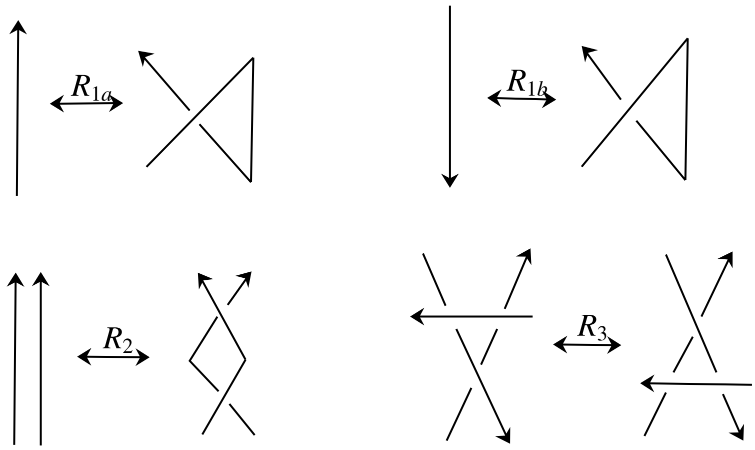

Figure 3. Oriented Reidemeister moves.

In Figure 3, we present a generating set of oriented Reidemeister moves. This set was proven to be minimal in [15]. The equivalence relation generated by oriented Reidemeister moves and local planar isotopies defines planar knotoids [11].

Remark 2.2. *The endpoints are considered fixed in the local region of the diagram where they lie, meaning that they are not allowed to cross over or under any arc of the diagram. Such moves, illustrated in Figure 4, are termed forbidden moves. In fact, if these moves were allowed, any knotoid could be deformed into a trivial knotoid.*

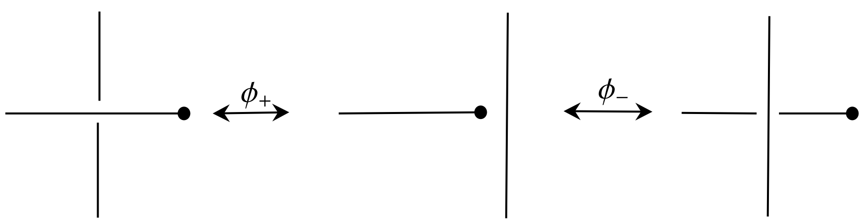

Figure 4. Forbidden moves.

Definition 2.3. *([7, 14]) A singular planar knotoid diagram is a planar knotoid diagram with finitely many transverse double points, disjoint from the endpoints and marked by solid dots. These double points are called singular crossings.*

Two singular planar knotoid diagrams are equivalent if and only if one can be obtained from the other by a finite sequence of the Reidemeister moves for singular planar knotoids shown in Figure 5 and planar isotopies, all performed away from the endpoints (see [7, 14]). The usual forbidden moves for planar knotoids are also forbidden for singular planar knotoids. An oriented singular planar knotoid is an equivalence class of oriented singular planar knotoid diagrams.

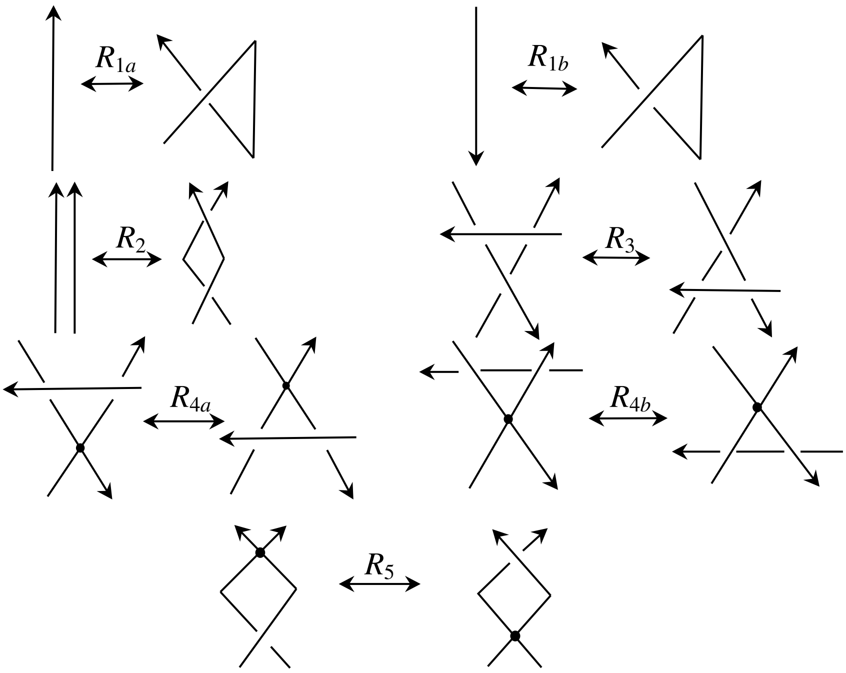

Figure 5. Singular Reidemeister moves.

Each double point of a singular oriented planar knotoid diagram D splits it into two oriented arcs. One of these arcs forms a closed curve, called the lobe of the singular point. The other arc is an open curve connecting the two endpoints of the knotoid. Because singular isotopies avoid the two endpoint punctures, the lobe determines a well-defined homology class and hence, a well-defined winding pair $(l(s), h(s))$. Note that this pair of winding numbers is not well-defined for spherical knotoids due to the isotopies of the sphere.

Remark 2.4. *A planar knotoid diagram may be regarded as a diagram in the twice-punctured plane, where the punctures are chosen in the regions containing the leg and the head. The lobe is considered as an oriented closed curve in the punctured plane. In this case, the pair $(l(s), h(s))$ can be regarded as an element of the first homology group of the plane with two punctures, which is $\mathbb{Z} \oplus \mathbb{Z}$ [11]. This element represents the lobe at the singular point s in the oriented singular planar knotoid D. The lobe determines a conjugacy class in the fundamental group $\pi_1(\mathbb{R}^2 \setminus \{p_{leg}, p_{head}\})$, which is the free group of rank two. In the present construction, we use only its abelianization $H_1(\mathbb{R}^2 \setminus \{p_{leg}, p_{head}\}; \mathbb{Z}) \cong \mathbb{Z} \oplus \mathbb{Z}$.*

Under a planar isotopy or a Reidemeister move supported in a disk disjoint from the endpoint punctures, corresponding lobes agree outside the disk and differ inside it by the boundary of a 2-chain *contained in that disk. Hence, their classes in* $H_1(\mathbb{R}^2 \setminus \{p_{\mathrm{leg}}, p_{\mathrm{head}}\}; \mathbb{Z})$ *and their ordered winding pairs are unchanged.*

Let D be an oriented planar knotoid diagram, and let c be a classical crossing. The 0-smoothing at c, also called smoothing against the orientation, is the local reconnection shown in Figure 6, where the two rows correspond to $\mathrm{sgn}(c) = +1$ and $\mathrm{sgn}(c) = -1$, respectively. More precisely, the 0-smoothing joins the two incoming local half-edges at c to each other and joins the two outgoing local half-edges to each other. Because the underlying knotoid diagram has a single open component, this reconnection again yields a single open component and creates no additional closed component. The arrows in Figure 6 determine the orientation of the smoothed component. Its initial and terminal endpoints are then taken as the leg and the head, respectively, of the resulting oriented planar knotoid diagram, which is denoted by D_c. Consequently, the two original endpoints may either retain or interchange their roles as the leg and the head.

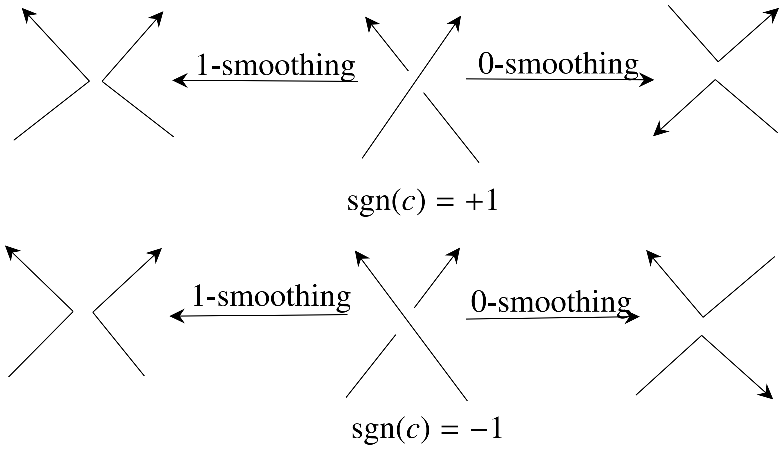

Figure 6. 0-smoothing and 1-smoothing.

Next, we review the affine index polynomial as given by Gügümcü and Kauffman in [4]. See also [16] for the origins of this invariant.

To define affine index weights, assign the label 0 to the initial arc, and propagate labels along the oriented diagram by the rule in Figure 7. For a crossing c, let a and b be the labels on the two incoming arcs shown there, and set

$$w_+(c) = a - (b + 1), \qquad w_-(c) = b - (a - 1), \qquad w_D(c) = w_{\mathrm{sgn}(c)}(c).$$

Changing the initial label by a constant does not change any crossing weight.

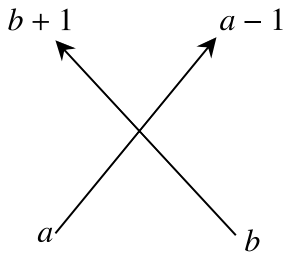

Figure 7. Integer labeling at a flat crossing.

Definition 2.5. *([4]) The affine index polynomial of a virtual or classical knotoid diagram D is defined by*

$$P_D(t) = \sum_{c \in C(D)} \operatorname{sgn}(c)(t^{w_D(c)} - 1),$$

where $C(D)$ denotes the set of all classical crossings of D. This polynomial is an invariant for both classical and virtual knotoids.

The same local labeling rule is often presented as Cheng coloring; Figure 8 records the relevant crossing conventions. Cheng and Gao [17] defined an integer index $\mathrm{Ind}(c)$ for each classical crossing of an oriented virtual knot by means of Cheng coloring. With the convention adopted here, $w_D(c)$ agrees with $\mathrm{Ind}(c)$, up to the global sign convention used in the cited source.

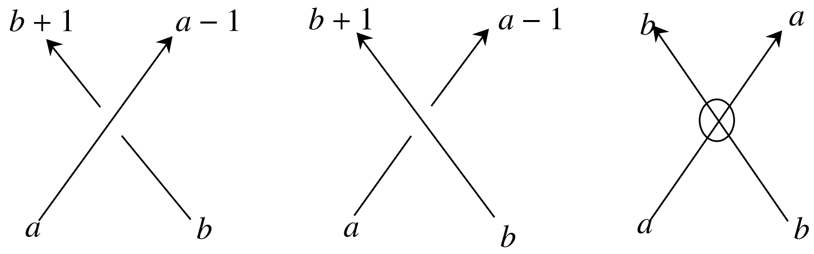

Figure 8. Cheng coloring of D.

3. The ordered winding Laurent polynomial

In this section, inspired by the affine index polynomial of knotoids introduced in [4], we define a polynomial invariant for planar knotoids using winding numbers. The construction is given as follows.

Definition 3.1. *Let D be an oriented planar knotoid diagram. We define the ordered winding Laurent polynomial $H_D(x, y)$ by*

$$H_D(x, y) = \sum_{c \in C(D)} \operatorname{sgn}_D(c) w_D(c)(x^{l_D(c)} y^{h_D(c)} - x^{-h_D(c)} y^{-l_D(c)}), \tag{3.1}$$

where $C(D)$ denotes the set of all classical crossings of D. The integers $l_D(c)$ and $h_D(c)$ are the winding numbers of the closed lobe around the leg and around the head, respectively, where the closed lobe is obtained by replacing the crossing c with a transverse double point and following the oriented closed component. Counterclockwise winding is taken to be positive and clockwise winding negative. Thus, $H_D(x, y) \in \mathbb{Z}[x^{\pm 1}, y^{\pm 1}]$.

The antisymmetric monomial difference in (3.1) is chosen so that reversing the orientation of the knotoid changes the ordered winding pair from $(l(c), h(c))$ to $(-h(c), -l(c))$ and reverses the sign of the bracket. This sign change compensates for the sign change of the affine index weight under orientation reversal. This compatibility will be used below to derive the orientation-reversal formula for $H_D(x, y)$.

Theorem 3.2. *The polynomial $H_D(x, y)$ is an invariant for oriented planar knotoids.*

Proof. For an R_1 move, the newly created crossing has affine index weight zero and therefore contributes zero. Existing crossings retain their signs, weights, and winding pairs.

For an R_2 move, the two new crossings have opposite signs, equal affine index weights, and identical ordered winding pairs; their contributions cancel. For each pre-existing crossing c before the move, let c' denote the corresponding crossing after the move. As shown in Figure 9, if the unique lobe obtained by resolving a crossing c into a double point contains one of the two arcs involved in the R_2 move, then the lobe obtained by resolving c' also contains one of these two arcs. If the lobe obtained by resolving c contains both arcs of the R_2 move, then resolving c' produces a lobe that contains a closed curve between c'_1 and c'_2. This closed curve does not affect the winding numbers around the leg and the head of the knotoid. Existing crossings preserve their data because the extra local bigon is null-homologous in the twice-punctured plane.

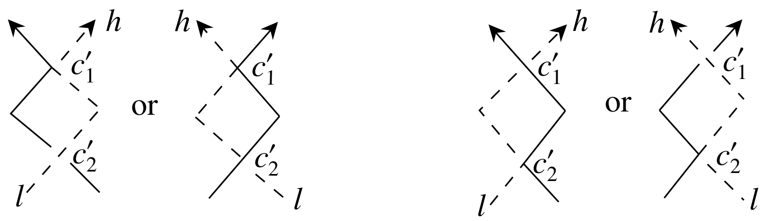

Figure 9. Resolving c'_1 or c'_2 into a double point.

Under an R_3 move, let D and D' denote the diagrams before and after the move. Let $\lambda_1, \lambda_2, \lambda_3$ be the integer labels on the three strands where they enter the Reidemeister disk. Propagating these labels by the Cheng rule determines all labels inside the disk. Along each strand, the same two signed label increments occur in D and D', although their order is interchanged. Hence, the three corresponding exit labels are identical, and all labels outside the disk coincide.

Let p, q, r be the three crossings of D in the Reidemeister disk, and let p', q', r' be their corresponding crossings in D'. Substituting the propagated labels into the formulas for w_+ and w_- gives

$$w_D(p) = w_{D'}(p'), \qquad w_D(q) = w_{D'}(q'), \qquad w_D(r) = w_{D'}(r').$$

The corresponding crossing signs are also unchanged under the oriented R_3 move.

For each corresponding pair $d \in \{p, q, r\}$ and $d' \in \{p', q', r'\}$, the lobes obtained by resolving d and d' agree outside the Reidemeister disk. Inside the disk, their difference is the boundary of a 2-chain contained entirely in the disk. Because the disk is disjoint from the endpoint punctures, the two lobes represent the same class in $H_1\big(\mathbb{R}^2 \setminus \{p_{\text{leg}}, p_{\text{head}}\}; \mathbb{Z}\big)$, and therefore have the same ordered winding pair. Thus, the three summands corresponding to p, q, r are preserved. All crossings outside the Reidemeister disk retain their signs, affine index weights, and ordered winding pairs. Hence, every summand in (3.1) is preserved, and $H_D(x, y)$ is invariant under the R_3 move. □

Remark 3.3. *The polynomial has the intrinsic antisymmetry*

$$H_D(y^{-1}, x^{-1}) = -H_D(x, y).$$

In particular, $H_D(1, 1) = 0$.

Proposition 3.4. *The polynomial* $H_D(x, y)$ *is invariant under an arbitrary crossing change. Consequently, it factors through the underlying oriented flat planar knotoid.*

Proof. At a switched crossing c, both $\mathrm{sgn}_D(c)$ and $w_D(c)$ change sign, whereas the ordered winding pair $(l_D(c), h_D(c))$ is unchanged. Hence, the product $\mathrm{sgn}_D(c)w_D(c)$ is unchanged, and the ordered winding pair is unchanged. Therefore, by (3.1), the summand corresponding to c is unchanged. The argument applies independently at every crossing. □

For any planar knotoid diagram D, let $-D$ denote the planar knotoid diagram with the reversed orientation. If D and $-D$ represent the same planar knotoid, then the planar knotoid is called invertible. The diagram $-D$ is called the inverse of D, as shown in Figure 10.

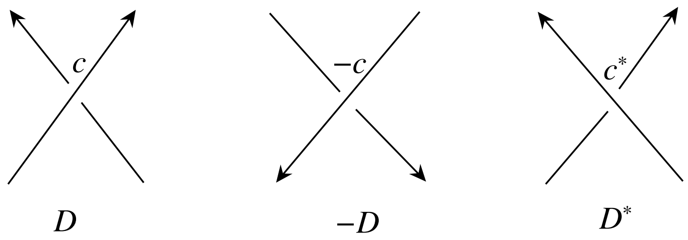

Figure 10. D, $-D$, and D^*.

For any planar knotoid diagram D, let D^* denote the planar knotoid diagram obtained by reversing the over/under information at all crossings of D while preserving its orientation. The diagram D^* is called the mirror image of D, as shown in Figure 10. If D and D^* are equivalent, then D is called amphicheiral; otherwise, it is called cheiral.

Proposition 3.5. *Let $-D$ be obtained by reversing the orientation of D, and let D^* be its mirror image. Then,*

$$H_{-D}(x, y) = H_D(x, y), \qquad H_{D^*}(x, y) = H_D(x, y).$$

Proof. Let $-c$ denote the crossing of $-D$ corresponding to a crossing c of D. Then,

$$\mathrm{sgn}_{-D}(-c) = \mathrm{sgn}_D(c), \quad w_{-D}(-c) = -w_D(c), \quad l_{-D}(-c) = -h_D(c), \quad h_{-D}(-c) = -l_D(c).$$

Consequently,

$$\begin{aligned}&\mathrm{sgn}_{-D}(-c)w_{-D}(-c)(x^{l_{-D}(-c)}y^{h_{-D}(-c)} - x^{-h_{-D}(-c)}y^{-l_{-D}(-c)})\\ &= \mathrm{sgn}_D(c)w_D(c)(x^{l_D(c)}y^{h_D(c)} - x^{-h_D(c)}y^{-l_D(c)}).\end{aligned}$$

Summing gives the first equality. For the mirror image,

$$\mathrm{sgn}_{D^*}(c^*) = -\,\mathrm{sgn}_D(c), \quad w_{D^*}(c^*) = -w_D(c), \quad l_{D^*}(c^*) = l_D(c), \quad h_{D^*}(c^*) = h_D(c),$$

so the product $\mathrm{sgn}(c)w_D(c)$ and the ordered winding pair are unchanged. This proves the second equality. □

4. The ordered winding smoothing polynomial

Although $H_D(x, y)$ records the affine index weights $w(c)$ and endpoint winding data at each crossing, it may vanish due to cancellations. The 0-smoothing construction below measures how $H_D(x, y)$ changes under local smoothing and can therefore retain information lost by $H_D(x, y)$ itself. Motivated by this observation, we define the following 0-smoothing polynomial for planar knotoids.

Definition 4.1. *For an oriented planar knotoid diagram D, let*

$$\mathrm{wr}(D) = \sum_{c \in C(D)} \mathrm{sgn}(c)$$

be the writhe. We define

$$F_D(x,y) = [\sum_{c \in C(D)} \mathrm{sgn}(c) H_{D_c}(x,y)] - \mathrm{wr}(D) H_D(x,y), \tag{4.1}$$

where $C(D)$ denotes the set of crossings of D, and D_c denotes the oriented planar knotoid diagram obtained from D by applying 0-smoothing at a crossing c. Thus, $F_D(x,y) \in \mathbb{Z}[x^{\pm 1}, y^{\pm 1}]$.

In each summand, exactly one crossing c of the original diagram D is smoothed. No successive or iterated smoothing is involved; hence, the definition contains no choice of smoothing order. The polynomial $F_D(x,y)$ is not intended to be a complete invariant. It may vanish for diagrams for which $H_D(x,y)$ is nonzero, and conversely the smoothing difference may be nonzero after cancellations make $H_D(x,y)$ vanish. Its role is therefore complementary: Section 4.1 proves a specific separation from the affine index polynomial and $H_D(x,y)$, but no universal dominance over other planar knotoid invariants is claimed.

Because $H_E(1,1) = 0$ for every oriented planar knotoid diagram E, Eq (4.1) also gives $F_D(1,1) = 0$. Thus, the natural evaluation $x = y = 1$ is trivial and does not recover a nontrivial knotoid or classical knot invariant. We do not establish any other specialization of $H_D(x,y)$ or $F_D(x,y)$ that recovers a previously known invariant.

Theorem 4.2. *The polynomial $F_D(x,y)$ is an invariant of oriented planar knotoids.*

Proof. We verify invariance under the classical Reidemeister moves.

For an R_1 move, assume that D' is obtained from D by introducing a crossing a' of type R_{1a} or a crossing b' of type R_{1b}. For each pre-existing crossing c of D, let c' be the corresponding crossing of D'. The smoothed diagrams D_c and $D_{c'}$ are related by the same R_1 move. Hence,

$$H_{D_c}(x,y) = H_{D'_{c'}}(x,y).$$

Moreover, as shown in Figure 11, $D'_{a'}$ is the inverse of D, whereas $D'_{b'}$ is equivalent to D. By Proposition 3.5,

$$H_{D'_{a'}}(x,y) = H_D(x,y), \quad H_{D'_{b'}}(x,y) = H_D(x,y).$$

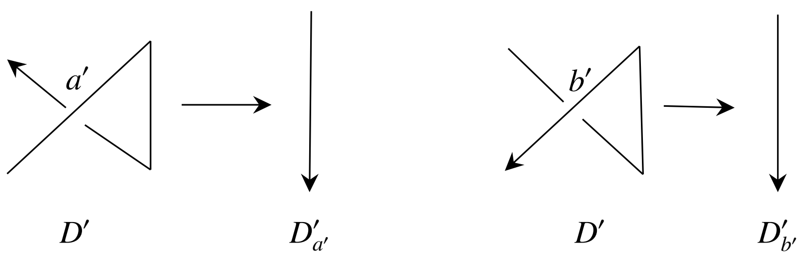

Figure 11. Left: the smoothing $D'_{a'}$; right: the smoothing $D'_{b'}$.

Write

$$\varepsilon = \mathrm{sgn}(a') \in \{+1, -1\}.$$

Because

$$H_{D'}(x,y) = H_D(x,y), \quad H_{D'_{a'}}(x,y) = H_D(x,y), \quad \text{and} \quad \mathrm{wr}(D') = \mathrm{wr}(D) + \varepsilon,$$

the cancellation is

$$\begin{aligned} F_{D'}(x,y) - F_D(x,y) &= \varepsilon H_{D'_{a'}}(x,y) - \big(\mathrm{wr}(D') - \mathrm{wr}(D)\big)H_D(x,y) \\ &= \varepsilon H_D(x,y) - \varepsilon H_D(x,y) = 0. \end{aligned}$$

The R_{1b} case is identical.

For an R_2 move, let c'_1 and c'_2 be the two crossings introduced in D', which have opposite signs, $\mathrm{sgn}(c'_1) = -\,\mathrm{sgn}(c'_2)$.

The smoothed diagrams $D'_{c'_1}$ and $D'_{c'_2}$ are related by R_1 moves, as shown in Figure 12. Hence,

$$H_{D'_{c'_1}}(x,y) = H_{D'_{c'_2}}(x,y).$$

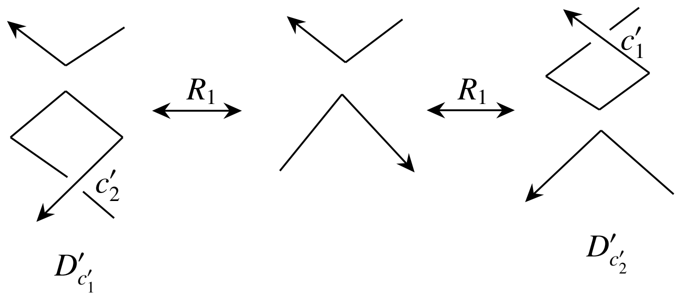

Figure 12. Left: the smoothing $D'_{c'_1}$; right: the smoothing $D'_{c'_2}$.

Putting $\varepsilon = \mathrm{sgn}(c'_1) = -\,\mathrm{sgn}(c'_2)$, their contributions cancel explicitly:

$$\varepsilon H_{D'_{c'_1}}(x,y) - \varepsilon H_{D'_{c'_2}}(x,y) = 0.$$

All other crossings correspond naturally, and their smoothed diagrams are related by an R_2 move. Because

$$H_{D'}(x,y) = H_D(x,y), \ \mathrm{wr}(D) = \mathrm{wr}(D'),$$

we obtain $F_{D'}(x,y) = F_D(x,y)$.

We next consider an R_3 move. Let $p,\ q,\ r$ be the three crossings of D involved in the move, and let $p',\ q',\ r'$ be the corresponding crossings of D'. If c is a crossing outside the local region of the R_3 move, and c' is its corresponding crossing in D', then D_c and $D'_{c'}$ are related by an R_3 move. Hence, $H_{D_c}(x,y) = H_{D'_{c'}}(x,y)$.

It remains to compare the smoothings at the three crossings involved in the move, as shown in Figure 13. For an oriented planar knotoid diagram E and a crossing d in $C(E)$, set

$$\phi_E(d) = \mathrm{sgn}_E(d) w_E(d) \left(x^{l_E(d)} y^{h_E(d)} - x^{-h_E(d)} y^{-l_E(d)} \right).$$

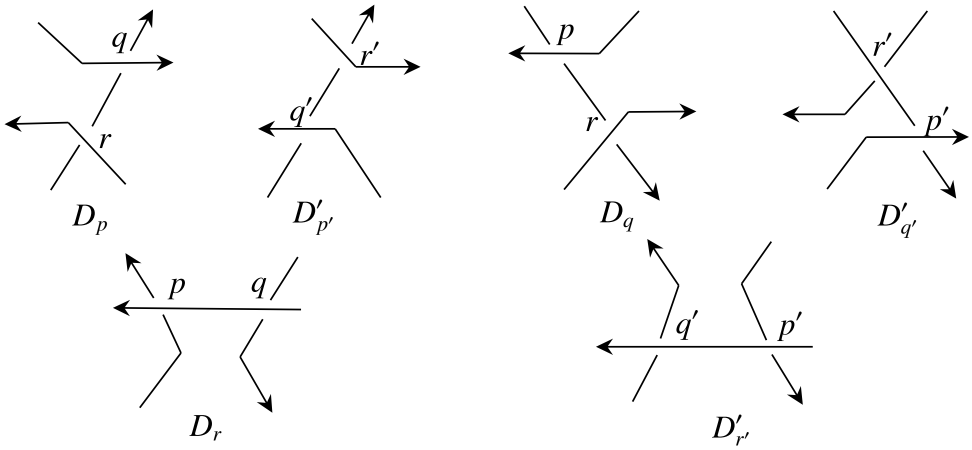

Figure 13. The three smoothing comparisons for the R_3 move: $(D_p, D'_{p'})$, $(D_q, D'_{q'})$, and $(D_r, D'_{r'})$.

Consider the Cheng labels induced on the six boundary arcs of the R_3 disk. By the propagation argument used in Theorem 3.2, these boundary labels agree before and after the move. After smoothing p and p', the remaining crossings q, r correspond to r', q', respectively. For each pair, the signs and affine weights agree, and the resolved lobes differ inside the endpoint-free disk by the boundary of a 2-chain. Thus, their ordered winding pairs agree, and

$$\phi_{D_p}(q) = \phi_{D'_{p'}}(r'), \qquad \phi_{D_p}(r) = \phi_{D'_{p'}}(q').$$

All crossings outside the disk retain the same labels and lobe classes, so $H_{D_p}(x, y) = H_{D'_{p'}}(x, y)$. When q and q' are smoothed, p, r correspond to r', p'. In the relevant local pair, both the crossing sign and the affine weight change sign, so their product is preserved; the lobe classes are again equal. Hence, $H_{D_q}(x, y) = H_{D'_{q'}}(x, y)$. The same argument gives $H_{D_r}(x, y) = H_{D'_{r'}}(x, y)$.

Because the corresponding crossings have the same signs, and

$$H_D(x, y) = H_{D'}(x, y), \qquad \mathrm{wr}(D) = \mathrm{wr}(D'),$$

all terms in the definition of $F_D(x, y)$ agree under the R_3 move. Therefore, $F_{D'}(x, y) = F_D(x, y)$.

Thus, $F_D(x, y)$ is an invariant of oriented planar knotoids. □

Next, we consider some properties of the polynomial $F_D(x, y)$.

Proposition 4.3. *Let $-D$ be obtained by reversing the orientation of D, and let D^* be its mirror image. Then,*

$$F_{-D}(x, y) = F_D(x, y), \qquad F_{D^*}(x, y) = -F_D(x, y).$$

Proof. Let c be a crossing in D and $-c$ the corresponding crossing in $-D$. Under the smoothing convention used here, reversing the diagram reverses the local smoothing orientation and simultaneously interchanges the roles of the leg and the head. These two changes compensate each other, so D_c and $(-D)_{-c}$ represent the same oriented planar knotoid, as shown in Figure 14. Thus, by Proposition 3.5 and the identities $\mathrm{sgn}_{-D}(-c) = \mathrm{sgn}_D(c)$ and $\mathrm{wr}(-D) = \mathrm{wr}(D)$, the first formula follows.

For the mirror image, $D^*_{c^*}$ is the inverse of D_c, as shown in Figure 14. Therefore, Proposition 3.5 gives $H_{D^*_{c^*}}(x, y) = H_{D_c}(x, y)$. Because all crossing signs and the writhe change sign, $\mathrm{sgn}_{D^*}(c^*) = -\,\mathrm{sgn}_D(c)$, and $\mathrm{wr}(D^*) = -\,\mathrm{wr}(D)$. This proves the second identity. □

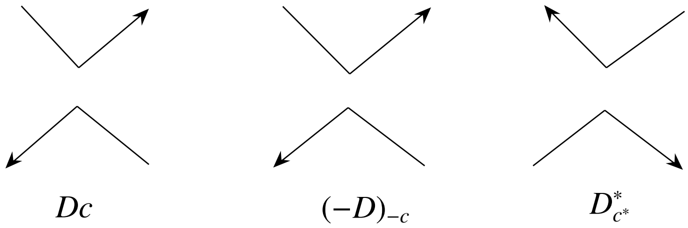

Figure 14. From left to right: D_c, $(-D)_{-c}$, and $D^*_{c^*}$.

Spherical knotoids admit a natural product operation given by concatenation. For any spherical knotoid diagrams D_1 and D_2, we may assume without loss of generality that the head of D_1 and the leg of D_2 lie in the exteriors of their respective diagrams. The product D_1D_2 is then defined by identifying the head of D_1 with the leg of D_2 in the disjoint union $D_1 \cup D_2$, as shown in Figure 15.

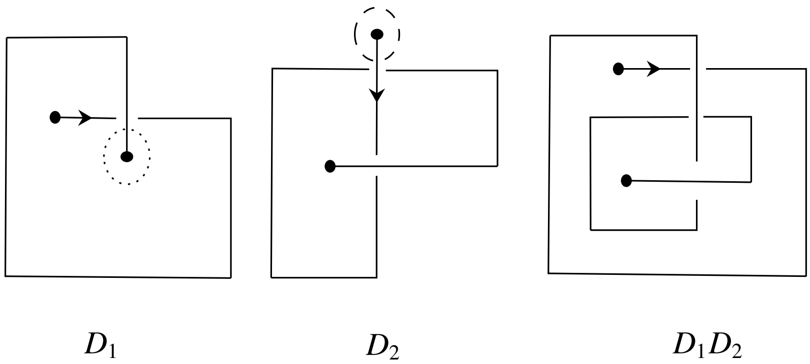

Figure 15. Product of D_1 and D_2.

For planar knotoids, the product is defined only after choosing a distinguished exterior region. For an actual planar drawing, the exterior region R_∞ is the unique unbounded component of $\mathbb{R}^2 \setminus D$. This differs from choosing an arbitrary complementary region of a spherical diagram and then declaring it to contain the point at infinity. We regard (D, R_∞) as the planar datum and require the leg of the second factor to be incident to its exterior region. This condition is essential for the formula below: Without it, a lobe in the second factor may acquire a different winding number about the product leg.

Definition 4.4. *([18]) Let $(D_1, R_{1,\infty})$ and $(D_2, R_{2,\infty})$ be planar knotoid diagrams, with the leg of D_2 incident to $R_{2,\infty}$. The product D_1D_2 is obtained by inserting a small copy of D_2 in the region of D_1 incident to its head and joining the leg of D_2 to that head by an embedded arc disjoint from both diagrams. The usual left and right drawings of this joining arc are isotopic inside that complementary region and therefore give the same planar product.*

Proposition 4.5. *Let $(D_1, R_{1,\infty})$ and $(D_2, R_{2,\infty})$ be planar knotoid diagrams for which the product D_1D_2 is defined, with the leg of D_2 lying in the distinguished exterior region $R_{2,\infty}$. Then,*

$$F_{D_1D_2}(x, y) = F_{D_1}(x, y) + F_{D_2}(x, y).$$

Proof. The product introduces no new crossings. Choose the initial Cheng label to be 0 at the leg of D_1. The labels induced on the copy of D_2 differ from its original labels by an additive constant, so all affine index weights are unchanged.

For a crossing of D_1, the head of D_2 lies in the same component of the complement of its lobe as the head of D_1. For a crossing of D_2, the leg of D_1 lies in the same exterior component as the leg of D_2. Hence, the ordered winding pairs are unchanged. Because the crossing signs are also unchanged,

$$H_{D_1D_2}(x,y) = H_{D_1}(x,y) + H_{D_2}(x,y).$$

Now, let $a \in C(D_1)$, and set

$$E_a = (D_1D_2)_a.$$

If the smoothing at a preserves the roles of the endpoints of D_1, the orientation of E_a passes through $(D_1)_a$ and then through D_2. If the smoothing exchanges these roles, the orientation passes first through D_2 in the reverse direction and then through $(D_1)_a$.

In the second case, the leg of E_a is the head of D_2, and its head is the leg of D_1. For a lobe inherited from $(D_1)_a$, the head of D_2 lies in the same component of its complement as the head of D_1. Therefore, its ordered winding pair is the same as that computed in $(D_1)_a$. For a lobe inherited from D_2, the leg of D_1 lies in the same exterior component as the leg of D_2. Therefore, its ordered winding pair is the same as that computed in $-D_2$. The Cheng labels on each part differ from the corresponding separate labeling by an additive constant. Thus, in either case,

$$H_{E_a}(x,y) = H_{(D_1)_a}(x,y) + H_{-D_2}(x,y) = H_{(D_1)_a}(x,y) + H_{D_2}(x,y),$$

where the second equality follows from Proposition 3.5.

Similarly, let $b \in C(D_2)$, and set

$$E_b = (D_1D_2)_b.$$

If the smoothing at b preserves the roles of the endpoints of D_2, the orientation of E_b passes through D_1 and then through $(D_2)_b$. If these roles are exchanged, the orientation passes first through $(D_2)_b$ and then through D_1 in the reverse direction.

For a lobe inherited from $(D_2)_b$, the leg of D_1 lies in the same exterior component as the leg of D_2, so its ordered winding pair is the same as that computed in $(D_2)_b$. For a lobe inherited from D_1, the head of D_2 lies in the same component of its complement as the head of D_1, so its ordered winding pair is the same as that computed in $-D_1$. Consequently,

$$H_{E_b}(x,y) = H_{-D_1}(x,y) + H_{(D_2)_b}(x,y) = H_{D_1}(x,y) + H_{(D_2)_b}(x,y),$$

again by Proposition 3.5.

Substituting these identities into (4.1) gives

$$\begin{aligned}
F_{D_1D_2}(x,y) = & \sum_{a\in C(D_1)} \operatorname{sgn}(a)H_{(D_1)_a}(x,y) + \operatorname{wr}(D_1)H_{D_2}(x,y) \\
& + \sum_{b\in C(D_2)} \operatorname{sgn}(b)H_{(D_2)_b}(x,y) + \operatorname{wr}(D_2)H_{D_1}(x,y) \\
& - (\operatorname{wr}(D_1) + \operatorname{wr}(D_2))\big(H_{D_1}(x,y) + H_{D_2}(x,y)\big) \\
= & \left[\sum_{a\in C(D_1)} \operatorname{sgn}(a)H_{(D_1)_a}(x,y) - \operatorname{wr}(D_1)H_{D_1}(x,y)\right]
\end{aligned}$$

$$+\left[\sum_{b\in C(D_2)} \operatorname{sgn}(b)H_{(D_2)_b}(x,y) - \operatorname{wr}(D_2)H_{D_2}(x,y)\right]$$
$$= F_{D_1}(x,y) + F_{D_2}(x,y).$$

This proves the result. □

4.1. *A family distinguished by $F_D(x,y)$*

Define D_0 to be the diagram in Figure 16 with the single crossing e_1 in the indicated twist band. For $n \geq 0$, having constructed D_n, define D_{n+1} by inserting one additional positive full twist in the same band, with the orientation and crossing information as shown in Figure 16. Label the two new crossings e_{2n+2} and e_{2n+3}, from bottom to top in the twist band. The crossings $c_1, \ldots, c_4$, the two endpoints, and all arcs outside the twist band are left unchanged. Thus, $C(D_n) = \{c_1, c_2, c_3, c_4, e_1, \ldots, e_{2n+1}\}$.

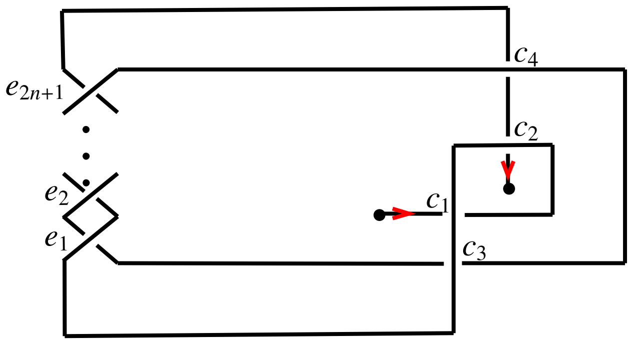

Figure 16. The planar knotoid D_n.

Start the Cheng labeling with label 0 at the leg. Applying the labeling rule to one added full twist shows that the ordered pair of labels entering the twist is recovered at its exit. Hence, by induction on n, the labels on the fixed part containing $c_1, \ldots, c_4$ are independent of n. At every crossing e_i, the incoming labels satisfy $a = b + 1$, and therefore,

$$w_{D_n}(e_i) = a - (b+1) = 0, \qquad 1 \leq i \leq 2n+1.$$

Direct application of the same labeling rule at the four fixed crossings gives

$$w_{D_n}(c_1) = -1, \qquad w_{D_n}(c_2) = 1, \qquad w_{D_n}(c_3) = w_{D_n}(c_4) = 0.$$

Moreover,

$$\operatorname{sgn}(c_1) = \operatorname{sgn}(c_2) = +1, \qquad \operatorname{sgn}(c_3) = \operatorname{sgn}(c_4) = -1,$$

and every e_i is positive. Therefore,

$$P_{D_n}(t) = \sum_{c\in C(D_n)} \operatorname{sgn}(c)(t^{w_{D_n}(c)} - 1)$$
$$= (t^{-1} - 1) + (t - 1)$$
$$= t + t^{-1} - 2,$$

which is independent of n.

The signs, affine index weights, ordered winding pairs, and contributions to $H_{D_n}(x,y)$ are summarized in Table 1.

Table 1. Crossing data for the planar knotoid D_n, where $1 \le i \le 2n+1$.

Crossing	$\mathrm{sgn}(c)$	$w_{D_n}(c)$	$(l_{D_n}(c), h_{D_n}(c))$	Contribution to $H_{D_n}(x,y)$
c_1	$+1$	-1	$(0,1)$	$x^{-1}-y$
c_2	$+1$	$+1$	$(-2,-1)$	$x^{-2}y^{-1}-xy^2$
c_3	-1	0	$(-1,-1)$	0
c_4	-1	0	$(-1,-1)$	0
e_i	$+1$	0	$(-1,-1)$	0

Substituting the data in Table 1 into (3.1), the only nonzero contributions to $H_{D_n}(x,y)$ come from c_1 and c_2. All other crossings have affine index weight zero. Hence,

$$H_{D_n}(x,y) = x^{-1} - y + x^{-2}y^{-1} - xy^2.$$

After smoothing c_1 or c_2 as shown in Figure 17, a direct application of the affine index labeling rule shows that every remaining crossing has affine index weight zero. Thus,

$$H_{(D_n)_{c_1}}(x,y) = H_{(D_n)_{c_2}}(x,y) = 0.$$

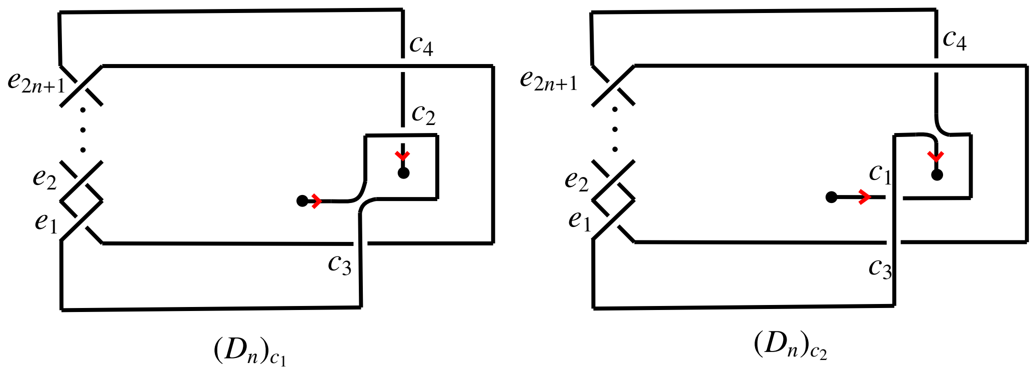

Figure 17. Left: $(D_n)_{c_1}$; right: $(D_n)_{c_2}$.

Let F denote the auxiliary knotoid diagram shown in Figure 18. We first justify the reduction of $(D_n)_{e_i}$. After applying the 0-smoothing at e_i, the remaining part of the twist band can be simplified by planar isotopy, and successive R_1 moves to the diagram F shown in Figure 18. The induced orientation of this diagram depends on the position of the smoothed crossing. Tracing the orientation through the twist band shows that it agrees with the orientation of F when i is even and is reversed when i is odd.

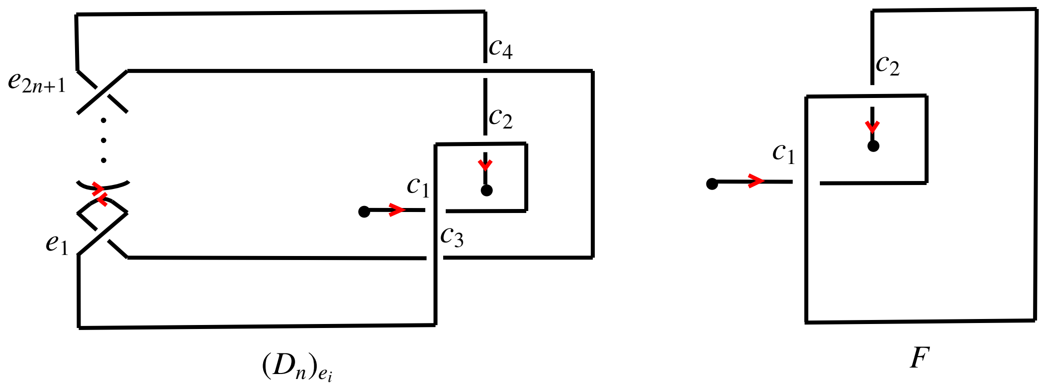

Figure 18. Left: $(D_n)_{e_i}$; right: the auxiliary diagram F.

For F, the two crossings with nonzero affine index weight satisfy

$$l_F(c_1) = l_F(c_2) = 0, \qquad h_F(c_1) = h_F(c_2) = 1,$$

and

$$\operatorname{sgn}_F(c_1)w_F(c_1) = -1, \qquad \operatorname{sgn}_F(c_2)w_F(c_2) = 1.$$

Their contributions to $H_F(x, y)$ cancel, so

$$H_F(x, y) = 0.$$

Because Proposition 3.5 gives

$$H_{-F}(x, y) = H_F(x, y),$$

we obtain

$$H_{(D_n)_{e_i}}(x, y) = 0, \qquad 1 \leq i \leq 2n + 1.$$

After smoothing c_3 or c_4 as shown in Figure 19, the resulting diagrams are related to $-F$ by R_1 moves. Thus,

$$H_{(D_n)_{c_3}}(x, y) = H_{(D_n)_{c_4}}(x, y) = H_{-F}(x, y) = 0.$$

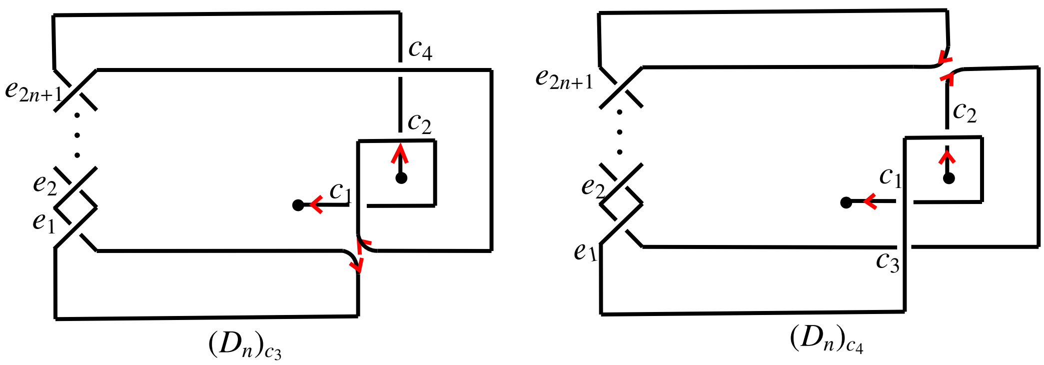

Figure 19. Left: $(D_n)_{c_3}$; right: $(D_n)_{c_4}$.

Because every smoothed H-polynomial appearing in (4.1) vanishes, and $\mathrm{wr}(D_n) = 2n+1$, we obtain

$$F_{D_n}(x,y) = -(2n+1)H_{D_n}(x,y) = -(2n+1)(x^{-1} - y + x^{-2}y^{-1} - xy^2).$$

For the first two members of the family, the preceding calculations give

$$P_{D_0}(t) = P_{D_1}(t) = t + t^{-1} - 2$$

and

$$H_{D_0}(x,y) = H_{D_1}(x,y) = x^{-1} - y + x^{-2}y^{-1} - xy^2.$$

Moreover,

$$\mathrm{wr}(D_0) = 1, \qquad \mathrm{wr}(D_1) = 3.$$

Because all the corresponding smoothed H-polynomials vanish, Eq (4.1) gives

$$F_{D_0}(x,y) = -H_{D_0}(x,y), \qquad F_{D_1}(x,y) = -3H_{D_1}(x,y),$$

which agrees with the general formula above.

For $m \neq n$,

$$F_{D_n}(x,y) - F_{D_m}(x,y) = -2(n-m)(x^{-1} - y + x^{-2}y^{-1} - xy^2) \neq 0.$$

Thus, the polynomial $F_D(x,y)$ distinguishes the diagrams D_n for distinct values of n, whereas both the affine index polynomial and $H_D(x,y)$ are independent of n.

5. Degree-one Vassiliev property

In this section, we review the definition of a Vassiliev invariant and prove that $F_D(x,y)$ is a degree-one Vassiliev invariant.

Let f be a planar knotoid invariant taking values in an abelian group, and let D be a singular planar knotoid with j singular crossings. We extend f to singular planar knotoids via the following recursive relation:

$$f^{(j)}(D) = f^{(j-1)}(D^+) - f^{(j-1)}(D^-),$$

where D^+ (resp. D^-) is the singular planar knotoid obtained from D by replacing a singular crossing with a classical crossing of sgn $= +1$ (resp. -1). For the initial condition, we set $f^{(0)} = f$.

Definition 5.1. *([7]) Let f be a planar knotoid invariant taking values in an abelian group. We say that f is a finite-type invariant (or Vassiliev invariant) of degree j if $f^{(j+1)}$ vanishes on all singular planar knotoids with $j+1$ singular crossings, and there exists a singular planar knotoid D with j singular crossings such that $f^{(j)}(D) \neq 0$. The smallest such non-negative integer j is called the degree of f.*

Corollary 5.2. *The invariant $H_D(x,y)$ is a nontrivial finite-type invariant of degree zero.*

Proof. By Proposition 3.4, the first Vassiliev difference $H_{D^+}(x,y) - H_{D^-}(x,y)$ vanishes at every singular crossing. Table 1 supplies diagrams for which $H_D(x,y) \neq 0$, so the invariant is nontrivial and has degree zero. □

Remark 5.3. *Because*

$$\mathrm{wr}(D) = \sum_{c\in C(D)} \mathrm{sgn}(c),$$

Eq (4.1) *can be rewritten as*

$$F_D(x,y) = \sum_{c\in C(D)} \mathrm{sgn}(c)(H_{D_c}(x,y) - H_D(x,y)).$$

Thus, $F_D(x,y)$ may be viewed as a signed smoothing transform of the crossing change invariant $H_D(x,y)$. The proof below uses both the crossing change invariance of $H_D(x,y)$ and its invariance under orientation reversal to eliminate the second Vassiliev difference. This suggests a possible broader construction for flat invariants satisfying analogous compatibility conditions. We do not formulate such a general theorem here.

Theorem 5.4. *The Laurent polynomial $F_D(x,y)$ is a degree-one Vassiliev invariant of planar knotoids.*

Proof. Let D have two singular crossings c_1, c_2, and let $D^{\alpha\beta}$ with $\alpha,\beta \in \{+1,-1\}$ denote the four classical resolutions. The underlying flat diagram and Cheng labels are the same for all four resolutions. Switching a resolved crossing changes both its sign and the selected affine index weight, so the product $\mathrm{sgn}(c_i)w(c_i)$ is unchanged. The winding pairs are unchanged, as well. Consequently,

$$H_{D^{++}}(x,y) = H_{D^{+-}}(x,y) = H_{D^{-+}}(x,y) = H_{D^{--}}(x,y).$$

The same conclusion holds after smoothing any crossing not equal to c_1, c_2. If one smooths c_i, the two choices of sign may induce opposite orientations of the open component, but Proposition 3.5 gives equal $H_D(x,y)$ values.

Let C_0 be the set of ordinary crossings of the singular diagram, and write $H_0(x,y)$ for the common value of the four polynomials $H_{D^{\alpha\beta}}(x,y)$.

For $d \in C_0$, put

$$S_d^{\alpha\beta}(x,y) = H_{(D^{\alpha\beta})_d}(x,y).$$

The four diagrams $(D^{\alpha\beta})_d$ differ only by crossing changes at c_1 and c_2. Hence, Proposition 3.4 shows that $S_d^{\alpha\beta}$ is independent of both signs; denote its common value by S_d.

After smoothing c_1, changing β produces only a crossing change at c_2, whereas changing α may reverse the global orientation of the resulting open component. Propositions 3.4 and 3.5 therefore give, respectively,

$$H_{(D^{\alpha+})_{c_1}}(x,y) = H_{(D^{\alpha-})_{c_1}}(x,y), \qquad H_{(D^{+\beta})_{c_1}}(x,y) = H_{(D^{-\beta})_{c_1}}(x,y).$$

Thus, all four values are equal; denote their common value by $S_{c_1}(x,y)$. Interchanging c_1 and c_2 gives a common polynomial $S_{c_2}(x,y)$.

If w_0 is the writhe of the ordinary crossings, then

$$\mathrm{wr}(D^{\alpha\beta}) = w_0 + \alpha + \beta.$$

Therefore,

$$\begin{aligned} F_{D^{\alpha\beta}}(x,y) &= \sum_{d\in C_0} \mathrm{sgn}(d)S_d + \alpha S_{c_1} + \beta S_{c_2} - (w_0 + \alpha + \beta)H_0(x,y) \\ &= Q_0 + \alpha Q_1 + \beta Q_2, \end{aligned}$$

where

$$Q_0(x,y) = \sum_{d\in C_0} \operatorname{sgn}(d) S_d(x,y) - w_0 H_0(x,y),$$
$$Q_1(x,y) = S_{c_1}(x,y) - H_0(x,y),$$
$$Q_2(x,y) = S_{c_2}(x,y) - H_0(x,y).$$

There is no $\alpha\beta$ term: Ordinary-crossing smoothings are independent of both resolutions; smoothing one singular crossing leaves only a crossing change at the other, and the writhe term is affine in α and β. Hence,

$$F_{D^{++}}(x,y) - F_{D^{+-}}(x,y) - F_{D^{-+}}(x,y) + F_{D^{--}}(x,y) = 0,$$

so the degree is at most one.

The two diagrams in Figure 20 differ only by switching the crossing c_1. Normalize the Cheng label on the initial arc to be zero. Propagating the labels along the orientation in Figure 20 gives $(a,b) = (0,0)$ at c_1 and $(a,b) = (1,-1)$ at c_2. The convention of Figure 7 then gives the affine index weights listed in Table 2. Because D^+ and D^- have the same underlying oriented flat diagram, their corresponding oriented lobes have the same ordered winding pairs:

$$(l(c_1), h(c_1)) = (0,-1), \qquad (l(c_2), h(c_2)) = (1,0).$$

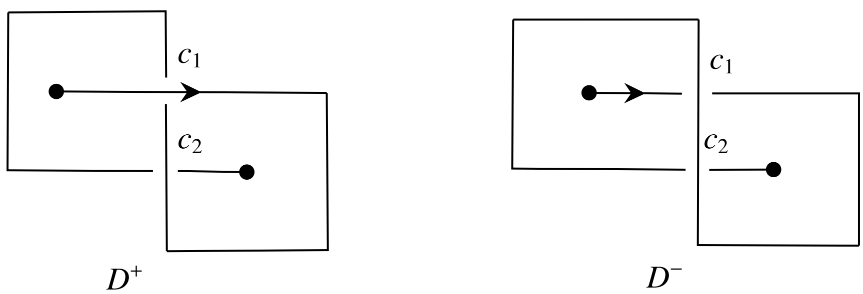

Figure 20. D^+ and D^-.

Table 2. Crossing data for the degree-one witness in Figure 20.

Diagram	Crossing	sgn	Incoming labels	w	(l,h)	H-term	Smoothed H
D^+	c_1	$+1$	$(a,b) = (0,0)$	-1	$(0,-1)$	$x - y^{-1}$	$H_{(D^+)_{c_1}} = 0$
D^+	c_2	-1	$(a,b) = (1,-1)$	-1	$(1,0)$	$x - y^{-1}$	$H_{(D^+)_{c_2}} = 0$
D^-	c_1	-1	$(a,b) = (0,0)$	$+1$	$(0,-1)$	$x - y^{-1}$	$H_{(D^-)_{c_1}} = 0$
D^-	c_2	-1	$(a,b) = (1,-1)$	-1	$(1,0)$	$x - y^{-1}$	$H_{(D^-)_{c_2}} = 0$

Substitution into Definition 3.1 shows that each crossing listed in Table 2 contributes $x - y^{-1}$; hence,

$$H_{D^+}(x,y) = H_{D^-}(x,y) = 2(x - y^{-1}).$$

After smoothing either c_1 or c_2, the resulting diagram has exactly one classical crossing. For a knotoid diagram with one classical crossing, let a and b be the incoming labels at its unique crossing as in

Figure 7. Between the two passages through this crossing, there is no other crossing, so the label is unchanged along the connecting arc. By the labeling rule in Figure 7, this gives $a = b+1$. Consequently,

$$w_+(c) = a - (b+1) = 0, \qquad w_-(c) = b - (a-1) = 0.$$

This implies that the remaining crossing has affine index weight zero, independently of its sign. Therefore,

$$H_{(D^+)_{c_1}}(x,y) = H_{(D^+)_{c_2}}(x,y) = H_{(D^-)_{c_1}}(x,y) = H_{(D^-)_{c_2}}(x,y) = 0.$$

Furthermore, $\mathrm{wr}(D^+) = 0$, and $\mathrm{wr}(D^-) = -2$. Therefore,

$$F_{D^+}(x,y) = 0, \qquad F_{D^-}(x,y) = 4(x - y^{-1}),$$

and

$$F_D^{(1)}(x,y) = F_{D^+}(x,y) - F_{D^-}(x,y) = -4(x - y^{-1}) \neq 0.$$

Thus, $F_D(x,y)$ has degree exactly one. □

6. Conclusions

In this paper, we introduced two Laurent polynomial invariants for oriented planar knotoids. The auxiliary polynomial $H_D(x,y)$ combines affine index weights with the ordered winding classes of crossing lobes in the twice-punctured plane, and the smoothing polynomial $F_D(x,y)$ records how this information changes under the 0-smoothing against the orientation, together with a writhe correction. We proved that both polynomials are invariant under planar knotoid equivalence. We also established their transformation rules under orientation reversal and mirror image and proved that $F_D(x,y)$ is additive under the planar product whenever the stated exterior region condition is satisfied.

The family D_n shows that the smoothing construction contains information not detected by the affine index polynomial or by $H_D(x,y)$, and the extension to singular planar knotoids shows that $F_D(x,y)$ is a Vassiliev invariant of degree exactly one. A natural limitation of the present construction is its dependence on affine index weights and on the abelianized winding class in

$$H_1(\mathbb{R}^2 \setminus \{p_{\mathrm{leg}}, p_{\mathrm{head}}\}; \mathbb{Z}).$$

Possible directions for further work include replacing the homology class by nonabelian fundamental group data, investigating iterated smoothing constructions that may yield higher-degree finite-type invariants, and comparing $F_D(x,y)$ systematically with other polynomial and homological invariants of planar knotoids.

The present definition is intrinsically planar: After passage to S^2, there is no fixed unbounded region, and the ordered endpoint winding pair is not preserved by spherical isotopy. A virtual extension would likewise require a replacement for the twice-punctured-plane winding class and a separate verification of the virtual Reidemeister moves. Although braidoids provide a diagrammatic connection between braids and planar knotoids [13], this article establishes no representation of bosonic, fermionic, or anyonic exchange statistics; such a physical interpretation would require additional structure beyond the invariants defined here.

Author contributions

Liang Liang: conceptualization, methodology, formal analysis, writing–original draft; Fangyu Jin: formal analysis, validation, writing–review and editing; Liyuan Ma: conceptualization, methodology, supervision, project administration, funding acquisition, writing–review and editing. All authors have read and approved the final version of the manuscript.

Use of Generative-AI tools declaration

The authors declare they have not used Artificial Intelligence (AI) tools in the creation of this article.

Acknowledgments

This work was supported by the Youth Foundation of Liaoning Normal University (No. LS2024Q003) and the Joint Project of Liaoning Provincial Science and Technology Plan (No. 2025-MSLH-431).

Conflict of interest

The authors declare that they have no conflicts of interest.

References

1. V. Turaev, Knotoids, *Osaka J. Math.*, **49** (2012), 195–223.
2. N. Gügümcü, S. Nelson, N. Oyamaguchi, Biquandle brackets and knotoids, *J. Knot Theory Ramifications*, **30** (2021), 2150064. https://doi.org/10.1142/S0218216521500644
3. N. Gügümcü, S. Nelson, Biquandle coloring invariants of knotoids, *J. Knot Theory Ramifications*, **28** (2019), 1950029. https://doi.org/10.1142/S0218216519500299
4. N. Gügümcü, L. H. Kauffman, New invariants of knotoids, *Eur. J. Combin.*, **65** (2017), 186–229. https://doi.org/10.1016/j.ejc.2017.06.004
5. K. Bataineh, New polynomial invariants of knotoids and the theory of polar knots, *Mediterr. J. Math.*, **19** (2022), 40. https://doi.org/10.1007/s00009-021-01974-4
6. A. Henrich, A sequence of degree one Vassiliev invariants for virtual knots, *J. Knot Theory Ramifications*, **19** (2010), 461–487. https://doi.org/10.1142/S0218216510007917
7. M. Manouras, S. Lambropoulou, L. H. Kauffman, Finite type invariants for knotoids, *Eur. J. Combin.*, **98** (2021), 103402. https://doi.org/10.1016/j.ejc.2021.103402
8. N. Gügümcü, L. H. Kauffman, Quantum invariants of knotoids, *Commun. Math. Phys.*, **387** (2021), 1681–1728. https://doi.org/10.1007/s00220-021-04081-3
9. S. Kim, Y. H. Im, S. Lee, A family of polynomial invariants for knotoids, *J. Knot Theory Ramifications*, **27** (2018), 1843001. https://doi.org/10.1142/S0218216518430010

10. Y. Feng, F. Li, The F-polynomial invariant for knotoids, *J. Knot Theory Ramifications*, **33** (2024), 2450032. https://doi.org/10.1142/S0218216524500329

11. K. Bataineh, F. Batayneh, A. H. Alkasasbeh, A new invariant of planar knotoids and finite-type invariants, *J. Knot Theory Ramifications*, **32** (2023), 2350077. https://doi.org/10.1142/S0218216523500773

12. D. Kutluay, *Winding homology of knotoids*, Ph.D. Thesis, Indiana University, 2020.

13. N. Gügümcü, L. H. Kauffman, S. Lambropoulou, A survey on knotoids, braidoids and their applications, In: C. C. Adams, C. M. Gordon, V. F. R. Jones, L. H. Kauffman, S. Lambropoulou, K. C. Millett, et al., *Knots, low-dimensional topology and applications*, Springer, 2019, 389–409. https://doi.org/10.1007/978-3-030-16031-9_19

14. K. Bataineh, M. Elhamdadi, M. Hajij, W. Youmans, Generating sets of Reidemeister moves of oriented singular links and quandles, *J. Knot Theory Ramifications*, **27** (2018), 1850064. https://doi.org/10.1142/S0218216518500645

15. M. Polyak, Minimal generating sets of Reidemeister moves, *Quantum Topol.*, **1** (2010), 399–411. https://doi.org/10.4171/QT/10

16. L. H. Kauffman, An affine index polynomial invariant of virtual knots, *J. Knot Theory Ramifications*, **22** (2013), 1340007. https://doi.org/10.1142/S0218216513400075

17. Z. Cheng, H. Gao, A polynomial invariant of virtual links, *J. Knot Theory Ramifications*, **22** (2013), 1341002. https://doi.org/10.1142/S0218216513410022

18. M. Elhamdadi, W. Moltmaker, M. Saito, Planar equivalence of knotoids and quandle invariants, *Topol. Appl.*, **369** (2025), 109407. https://doi.org/10.1016/j.topol.2025.109407